Heterogeneity of Brønsted Acidic Sites in Faujasite Type Zeolites due to Aluminum Content and Framework Structure

Marek Sierka,[†] Uwe Eichler,[†] Jerzy Datka,[‡] and Joachim Sauer*,[†]

Arbeitsgruppe Quantenchemie, Humboldt Universität zu Berlin, Institut für Chemie, Jägerstrasse 10/11, D-10117 Berlin, Germany, and Faculty of Chemistry, Jagiellonian University, ul. Ingardena 3, 30-060 Krakow, Poland

Received: March 30, 1998; In Final Form: June 3, 1998

The effect of Al for Si substitutions in the tetrahedral sites of the faujasite framework with low and high aluminium content on the properties of Brønsted sites is investigated by computational techniques. A combined quantum mechanics−interatomic potential functions approach (QM-Pot.) is applied which uses periodic boundary conditions and treats the whole zeolite structure. Both the Hartree−Fock and the density functional (B3LYP) methods are employed. Energies of deprotonation, O−H stretching harmonic frequencies, and ^{1}H NMR chemical shifts are calculated. In the first approximation, the acidity of Brønsted sites measured by the deprotonation energy is determined by the number of nearest neighbor Al atoms of the Si atom in the Al−O(H)−Si bridge, while the O−H stretching frequency and ^{1}H chemical shift depend on their crystallographic position. Beyond this, the ^{1}H NMR chemical shifts show a strong dependence on the overall lattice composition. There is no correlation between ^{1}H NMR chemical shifts and deprotonation energies; however, a linear relation between ^{1}H NMR chemical shifts and OH vibrational frequencies is supported.

1. Introduction

Zeolite catalysts of different framework structure or of different chemical composition show very different activity in many catalytical reactions.[1] They may also differ in the spectroscopic characteristics of their catalytically active sites.[1] We are interested in the heterogeneity of Brønsted acidic sites within a given framework and examine the simple and frequently studied faujasite type zeolites. Using *n*-butylamine as a titration agent Beaumont and Barthomeuf[2,3] have shown that the faujasites with Si/Al > 4.5 are characterized by a single type of strongly acidic sites and that the increase of the Al content above Si/Al = 4.5 results in the formation of sites of weak and intermediate acidity. For the isooctane[4] and *n*-hexane[5] cracking reactions the catalytic activity per Al atom of faujasites remains constant for Si/Al > 4.5 but decreases with increasing Al content for Si/Al < 4.5. A dependence on the Al content was also observed for the O−H stretching vibrational frequency of the Brønsted acidic sites. The IR spectrum of a H-faujasite (Si/Al = 20.7) shows two distinct O−H bands,[6] the so-called high-frequency (HF) band at 3623 cm^{-1} and the low-frequency (LF) band at 3550 cm^{-1}. They are assigned to acidic sites in two different crystallographic positions:[7] O_1H with the proton pointing into the large supercage and O_3H with the proton located inside the sodalite cage. These bands shift to lower frequencies with increasing Si/Al ratio.[6,7] It has been suggested that on adsorption of aromatic hydrocarbons the HF band (O_1H) of Na−HY with Si/Al = 2.56 splits into three submaxima,[8] indicating the presence of O_1H sites with different properties. Some authors believe that the HF band can be resolved into as many as seven submaxima, each belonging to an O_1H group with different Al environments.[9] The ^{1}H NMR spectrum of the HY zeolite with Si/Al = 2.6 shows a line at 3.9 ppm and a shoulder at 4.6 ppm which are assigned to O_1H and O_3H groups, respectively.[10] The O_1H peak shifts with increasing Si/Al ratio from 3.8 ppm (Na−HX zeolite, Si/Al = 1.2) to 4.4 ppm (HY zeolite, Si/Al = 10) but remains constant for Si/Al > 10.[11,12]

These observations were rationalized essentially in two ways. One assumption is that the activity decreases with the increasing number of the next nearest neighbor (NNN) Al atoms with respect to the Al atom of the bridging Al−O(H)−Si site (e.g. refs 13−15).

The following formula illustrates that among all NNN Al sites (T and T′) those are distinguished (T) that are the nearest tetrahedral neighbors of the Si atom of the Al−O(H)−Si bridge.

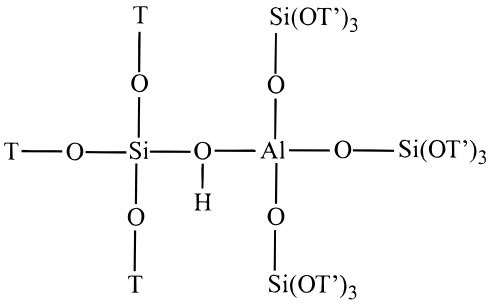

An isolated Brønsted site implies the existence of an Si atom with only one Al in its first neighbor tetrahedral sites. This is denoted Si(1Al). Increasing the Al content increases the number of NNN Al in general but also the number of Al atoms in nearest neighbor positions of the Si in the Al−O(H)−Si site, creating Si(2Al), Si(3Al), and Si(4Al) sites. The Al atoms in the first coordination sphere of the Si atom (T position) have the shortest distance to the acidic hydroxyl group among all the NNN Al atoms. This implies the following order for the activity: Si-

* To whom all correspondence should be addressed. E-mail: js@qc.ag-berlin.mpg.de.
† Humboldt Universität zu Berlin.
‡ Jagiellonian University.

S1089-5647(98)01670-8 CCC: $15.00
Published on Web 07/29/1998

(4Al) < Si(3Al) < Si(2Al) < Si(1Al). Experiments have been performed to confirm this model.[8,14,16]

The second explanation relates the acidic properties of zeolites to the mean Sanderson electronegativity.[17] It is based on the observation that many properties which show discontinuities when plotted against the aluminium content are linear functions of the mean electronegativity.[17−19]

The present study examines the influence of the Al content on the Brønsted acidity and the spectroscopic properties of OH groups in two different crystallographic positions of the faujasite framework, specifically on the O−H stretching harmonic frequencies and ^{1}H NMR chemical shifts. We consider O_1H and O_3H Brønsted sites and a wide range of different Si/Al ratios. The use of theoretical tools allows to separate the two different factors, framework position and Al content. As a measure of acidity we use the energy of deprotonation which is easily obtained by quantum chemical calculations.[20] It has been directly measured only for gas-phase molecules, while for surface hydroxyl groups inferences have been made from O−H frequency shifts.[21,22]

We apply a novel computational method[23,24] which combines the accurate quantum mechanical (QM) description of the site of interest, e.g. the Brønsted site, with the description of the periodic lattice by interatomic potential functions (Pot.). This QM-Pot. method is an "embedded" cluster type approach and provides substantial improvement over the traditional finite cluster approach.[25] The latter cuts a part of interest out of the periodic system and treats it as a molecule. It has several disadvantages, such as neglect of the long-range interactions and of structure constraints by the periodic system. Such cluster models are therefore unable to discriminate between active sites in different crystallographic positions or in different frameworks. Full periodic ab initio calculations which do not have such limitations are still computationally very demanding and can be performed only for systems of modest size and high symmetry. In contrast, the QM-Pot. method properly accounts for the structure of the periodic lattice and the long-range interactions at modest computational expense. We employ both the Hartree−Fock (HF) and density functional (DFT) methods and compare the results. The latter includes electron correlation effects.

2. Choice of Cluster Models

The notation *n* NNN Al is adopted for a structure with *n* next nearest neighbor Al atoms around the Al of the Al−O(H)−Si bridge, while Si(*n*Al) denotes a structure with *n* nearest neighbor Al atoms around the Si atom of this bridge. We use several types of embedded quantum mechanical cluster models. The first consists of two TO_4 tetrahedra only, represents a single Brønsted site, and is denoted 2T cluster (Figure 1a,b). Depending on the position of the lattice at which it is embedded, it models either the O_3H or the O_1H site (Figure 1a,b). The second, a four-membered silicate ring, is a characteristic building unit of the faujasite lattice. It includes one or two Al atoms and is used to compare isolated (4T-1Al model) with "paired" Brønsted sites (4T-2Al model). The Al atoms of these paired sites are next nearest neighbors (NNN) as far as their arrangement in tetrahedral lattice positions is concerned. Parts c and d of Figure 1 show the two cluster models and their position within the lattice. We use these 4T models for the O_1H position only. An interesting problem arises when embedding the 4T-1Al model (Figure 1c). Although in the faujasite lattice all the tetrahedral atoms are crystallographically equivalent, representing part of the framework by the cluster in the embedding

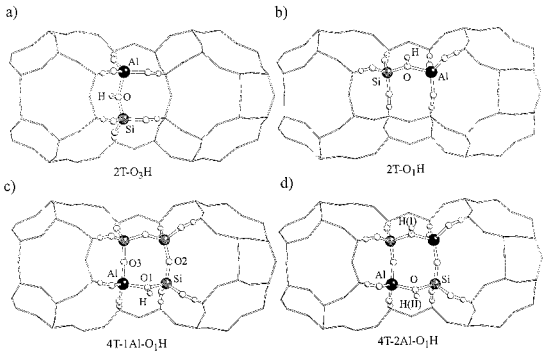

Figure 1. 2T and 4T cluster models and their positions in the framework.

scheme breaks this symmetry. There exist two distinct possibilities for embedding the 4T-1Al cluster into the framework so that its bridging OH group corresponds to the O_1H lattice position. In the first case the nonprotonated oxygen of the Al−O−Si bridge of the cluster is in the O_2 position, while in the second one it is in the O_3 position. In principle, the two positions of the cluster in the framework can lead to different bond distances and angles and, hence, to different computed properties of the same bridging hydroxyl group. Only in the limiting case in which the embedding potential perfectly mimics the fully periodic quantum mechanical potential energy surface, identical results for the two models are obtained. This provides the opportunity to check the accuracy of the combined QM-Pot. method applied. Our calculations show negligible deviations between structures, deprotonation energies, IR frequencies, and ^{1}H NMR shifts calculated for these two possible orientations of the 4T-1Al cluster. This is a strong argument for the reliability of the embedding method.

The clusters are embedded into the primitive cell of faujasite which consists of two sodalite cages joined through a hexagonal prism (48 TO_2 units; see Figures 1 and 3). We consider basically two different levels of Al content in the unit cell, low (high-silica material, Si/Al ≥ 23) and high (HY, Si/Al ≈ 2.43−3.0). For the high-silica material we examine the isolated Brønsted site, 0 NNN Al and Si(1Al), in a lattice containing only one acidic site per primitive cell (Si/Al = 47), and paired Brønsted sites, 1 NNN Al and Si(2Al), in a lattice with two sites per primitive cell (Si/Al = 23). The isolated site is modeled by the 4T-1Al (Figure 1c) and 2T clusters (Figure 1a,b). Schröder and Sauer[26] have shown by calculations that there is, in accord with the Löwenstein rule, a preferred way to distribute the two Al atoms in the H-faujasite lattice—the two Al atoms occupy two next nearest neighbor tetrahedral sites in four-membered rings, as shown in Figure 1d. The resulting negative charge is compensated for by the two protons forming two bridging hydroxyl sites. In principle, there exist 16 possibilities for distribution of the protons over the 8 oxygens of the two AlO_4 tetrahedra. Those with two protons on the central SiO_4 tetrahedron will have high energies. Among the low-energy distributions we consider the pattern with two protons at the O_1 positions. This structure is represented by our 4T-2Al cluster model.

To study the convergence properties of our QM-Pot. approach, we use an additional type of cluster models for the high-silica case. They are constructed by adding to each tetrahedral atom of the embedded 4T model a complete shell of SiO_4 tetrahedra. If two terminating hydroxyl groups are pointing to the same silicon atom of the outer region, this silicon atom is also included in the cluster and terminated with hydroxyl groups. The resulting clusters consist of 14 tetrahedral atoms and are

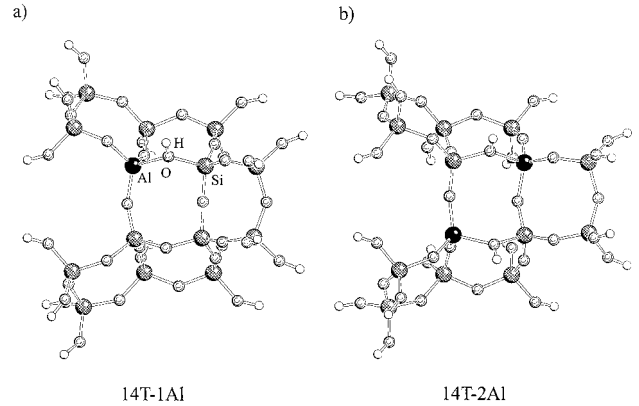

Figure 2. Large 14T-1Al and 14T-2Al cluster models.

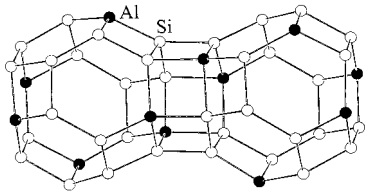

Figure 3. Al distribution in the faujasite lattice for Si/Al = 3.0. For simplicity oxygen atoms are omitted.

denoted 14T-1Al and 14T-2Al (Figure 2a,b, respectively). The additional structure relaxation effects were found to be negligible for such models,[24] and therefore only single point calculations are made on the structures optimized for the embedded 4T models.

To model the low Si/Al ratios typical of HY zeolites, the Al atoms are distributed over the lattice sites, as suggested by Klinowski et al.,[27] and the resulting negative charge is compensated for by distributing protons over the different oxygen sites. We choose two different proton occupation patterns O_1:O_2:O_3:O_4 = 8:2:4:0 (Si/Al = 2.43) and O_1:O_2:O_3:O_4 = 7:2:3:0 (Si/Al = 3). They are close to the populations deduced for zeolite Y (Si/Al = 2.43) from neutron powder diffraction experiments.[28] Figure 3 shows the Al distribution for Si/Al = 3. These structures are used for embedding 2T (Si/Al = 2.43), 4T-1Al, and 4T-2Al (Si/Al = 3) cluster models. For the framework with Si/Al = 2.43, the 2T cluster is used to model O_1H sites with different environments. They are labeled according to the type of Si atom in the Al−O(H)−Si bridge. The $\{2T\}_{2Al}$ and $\{2T\}_{3Al}$ clusters represent Si(2Al) and Si(3Al) sites, respectively. The *n*Al subscript outside the braces refers to the number of nearest neighbor Al atoms of the embedded Si atom, regardless of whether they are within the cluster or not. The Si atoms of the 2T models representing the O_3H site have either one or two nearest Al neighbors. They are denoted $\{2T\}_{1Al}$ and $\{2T\}_{2Al}$. There are two different $\{2T\}_{2Al}$ models for O_1H and three for O_3H sites with different configurations of the NNN Al atoms (Figure 4), denoted $\{2T\}_{2Al}(1)$−$\{2T\}_{2Al}(3)$. In the 4T models the nearest neighbor Al atoms of Si are explicitly included in the cluster. Hence, the 4T-1Al and 4T-2Al models represent Si(1Al) and Si(2Al) situations, respectively.

Figure 4 shows the topology of the NNN Al atoms of the Brønsted sites investigated in the low-silica faujasites. There are differences in the number of NNN Al beyond those emerging from the Si(*n*Al) count. Table 1 shows the specification of the embedded clusters used.

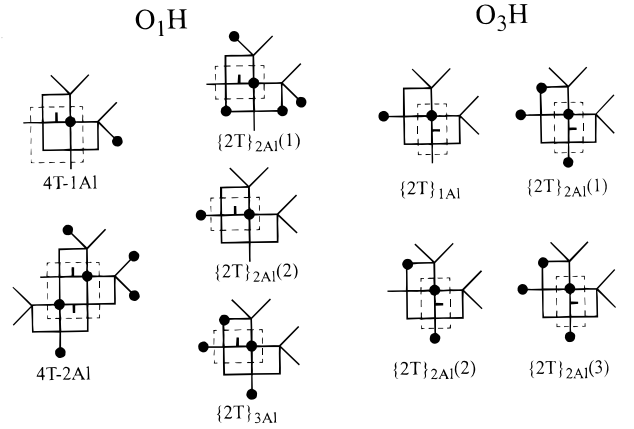

Figure 4. NNN Al distribution around Brønsted sites studied in the low-silica faujasites. For simplicity oxygen atoms are omitted. Investigated bridging hydroxyl groups are represented as small bars. Dashed rectangles indicate the positions of embedded clusters.

TABLE 1: Si/Al Ratios of Embedding Frameworks, Cluster Models, and QM Methods Used

type of faujasite	Si/Al	type of site: isolated	type of site: paired	QM method
high-silica	47	2T		HF
	47, 23	4T-1Al	4T-2Al	DFT, HF
	47, 23	14T-1Al	14T-2Al	DFT
HY	2.43	$\{2T\}_{1Al}$	$\{2T\}_{2Al}$, $\{2T\}_{3Al}$	HF
	3	4T-1Al	4T-2Al	DFT

3. Methods Used

3.1. Combined QM-Pot. Calculations. The present implementations[23,29] of the embedding scheme[23,24] use the GULP[30] program for the lattice energy minimization and the TURBOMOLE[31,32] program for the quantum mechanical calculations. The potential functions for the HF and DFT QM-Pot. calculations are shell-model ion-pair potentials with parameters derived from HF[33] and DFT[34] cluster calculations, respectively. The DFT calculations employ the B3LYP correlation-exchange functional.[35] The terminating hydrogen atoms of the cluster models are kept at a fixed distance from the oxygen atoms they terminate.[24,34] All combined QM-Pot. optimizations are performed without any symmetry constraints; i.e. the P_1 space group is assumed. The unit cell parameters are fixed to values found by a lattice energy minimization using the embedding shell-model potential alone. In the combined QM-Pot. scheme the atoms are relaxed until the largest Cartesian gradient component and the root mean square gradient are less than 0.0005 $E_h\ a_0^{-1}$.

Double-ζ plus polarization basis sets are used for aluminium, silicon, and hydrogen, while for oxygen atoms a triple-ζ plus polarization basis set is applied. This combination is labeled the T(O)DZP set. For the HF calculations on the 2T cluster models the (11s,7p/9s,5p/4s) Gaussian basis sets for Si,Al/O/H are taken from Huzinaga's tables.[36] The polarization functions have the following exponents: 0.4 (Si), 0.3 (Al), 1.2 (O), and 0.8 (H). These are the basis sets used in many previous studies from this laboratory, e.g. refs 23, 24, and 33. The HF and DFT calculations on 4T-1Al and 4T-2Al clusters are performed using the fully optimized basis sets from Ahlrichs' group.[37] The same polarization functions are added with the exception of a small change of the exponent for Al which is now 0.35. For numerical integration we use grid 3 from ref 32.

3.2. OH Frequencies and ^{1}H NMR Chemical Shifts. The O−H stretching force constants are calculated numerically using

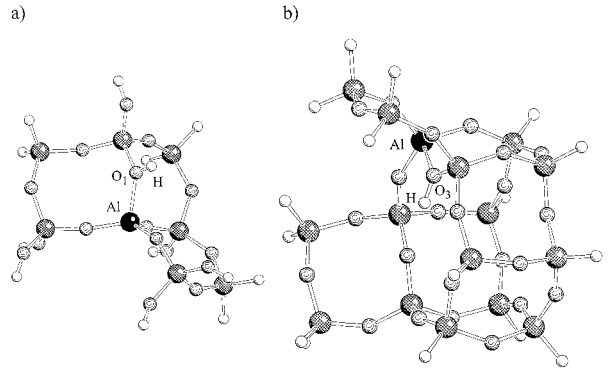

Figure 5. Cluster models used to calculate ^{1}H NMR shifts: (a) O_1H model, three fused four-membered silicate rings; (b) O_3H model, double six-membered silicate ring with two four-membered rings.

five points (step size, 1 pm) on the energy curve for the O−H bond.[24] We use force constants obtained by the QM method at the equilibrium structure found by the embedding, i.e. combined QM-Pot. technique. It is known[38] that such an approach can lead to improved results since an improved bond distance is used and harmonic frequencies are, in first approximation, determined by the bond distance. It is well-known that the HF method yields harmonic stretching frequencies that are systematically too large, while the DFT method nearly reproduces observed frequencies. For a better comparison with the experiment the HF frequencies have been scaled by the common factor 0.89, while DFT frequencies have been scaled[39] by a factor of 0.9716. We obtained this factor by comparison of the DFT frequencies for water and methanol with the corresponding experimental values. Note that this crude scaling procedure accounts also for anharmonicities since calculated harmonic frequencies are compared with observed fundamentals.

The calculations of the NMR shielding constants are done for clusters cut out of optimum periodic structures obtained by the combined QM-Pot. scheme. The size of the cluster proved crucial for obtaining reliable chemical shifts.[24] We use the clusters that yielded converged values for ^{1}H NMR shifts before.[24] For the O_1H position they consist of three joined four-membered silicate rings (8 TO_4 units), while for the O_3H site they consist of as many as 16 TO_4 units (Figure 5a,b, respectively). The calculations of the NMR shielding constants are performed within the coupled perturbed Hartree−Fock approach (CPHF) using a gauge including atomic orbitals (GIAO)[40] as implemented in the SHEILA[41] module of the TURBOMOLE program.[31] The TZP basis sets from Ahlrichs' group[37] are used on all of the atoms. The total number of basis functions was 770 for the O_1H and 1108 for the O_3H cluster models. The ^{1}H NMR chemical shifts with respect to tetramethylsilane (TMS), δ_{TMS}, are calculated from the absolute shielding constants, σ, using methanol as an internal secondary standard:[42]

$$\delta_{TMS}(\text{cluster}) = \delta_{TMS}(CH_3OH) + \sigma(CH_3OH) - \sigma(\text{cluster})$$

The absolute SCF shielding constants $\sigma(CH_3OH)$ are 32.71 and 31.79 ppm calculated at the HF and DFT B3-LYP optimized structures, respectively. The experimental gas-phase value $\delta_{TMS}(CH_3OH)$ is 0.02 ppm.[43]

3.3. Deprotonation Energies. They are calculated as the difference of the combined QM-Pot. energies of deprotonated and protonated structures according to the hypothetical reaction

$$Z{-}OH \rightarrow Z{-}O^- + H^+$$

If the QM cluster is large enough, the total reaction energy can be approximately written as[24]

$$\Delta E_{QM-Pot.} = \Delta E_{QM//QM-Pot.} + \Delta E_{LR//QM-Pot.}$$

The first term describes the QM part only, which is different from the free space cluster result because the structures of the embedded clusters are different from those of the free space clusters. The second term describes the correction due to the long-range crystal potential.

Two problems arise when applying periodic boundary conditions to a deprotonation reaction.[24] First, the calculation of the energy of a negatively charged unit cell is not possible using the traditional Ewald summation technique because of the infinite Coulomb repulsion. This problem is avoided by applying a neutralizing homogeneous background charge distribution.[44,45] Second, by taking the difference between QM-Pot. energies of the neutral and deprotonated zeolites, the energy for removing the proton from every unit cell is obtained. We are interested in the proton removal from a single acidic site. The energy for this process can be obtained by removing the interaction between the charged defects in the anionic unit cells. We follow the method proposed by Leslie and Gillan.[44] Details about the implementation are given elsewhere.[24]

4. Results and Discussion

We do not provide all structure data. We are rather interested in the structure relaxation upon deprotonation of the bridging hydroxyl groups. Table 2 shows changes of relevant distances and bond angles. Substantial but consistent changes are predicted at both DFT and HF levels. When the proton is removed, the Al−O and Si−O bonds become shorter by about 16 and 14 pm, respectively. The Al−O−Si bond angle increases by about 10°. In agreement with the results of previous calculations[24] the relaxation is generally larger for the O_3H than for the O_1H position in lattices of similar Si/Al ratios.

Tables 3 and 4 show the deprotonation energies, O−H stretching frequencies, and ^{1}H NMR chemical shifts. The deprotonation energies are decomposed into the contribution from the quantum chemical cluster calculation (QM//QM-Pot.) and a long-range electrostatic contribution from the shell-model potential (LR//QM-Pot.) as described in section 3.3. Both are calculated for the parent and deprotonated systems at their respective equilibrium structures obtained with the combined QM-Pot. approach. Sauer has suggested[46] removing the main body of the systematic error from calculated deprotonation energies by adding a constant value for a class of systems which is typical for a given method.[46] For the HF method with the T(O)DZP basis set a correction of −46 kJ/mol was obtained.[46,47] For the DFT(B3LYP) results with this basis set no correction is required due to a fortunate error compensation.[34] For comparison with experimental heats of deprotonation, we have to add nuclear motion corrections which have been estimated previously as −35 kJ/mol.[47] The final results show excellent agreement between values calculated for different cluster sizes and with different methods (HF and DFT). For the isolated O_1H site in a faujasite with Si/Al = 47 the values calculated at the HF and DFT levels using the 4T-1Al model (1169 and 1163 kJ/mol) and calculated at the HF level using the 2T model (1169 kJ/mol) agree within 6 kJ/mol. We may then expect that deprotonation energies obtained for different systems studied are directly comparable.

Further, the calculated deprotonation energies are remarkably stable when extending the quantum part of the model from 4T

TABLE 2: Structure Relaxation upon Deprotonation of the Bridging Hydroxyl Sites (Distances, pm; angles, deg)

			HF			DFT		
site	lattice Si/Al	cluster	$-\Delta$(Al−O)	$-\Delta$(Si-O)	$\Delta(\angle$Si−O(H)−Al)	$-\Delta$(Al−O)	$-\Delta$(Si-O)	$\Delta(\angle$Si−O(H)−Al)
O_1H	47/23	4T-1Al	17.1	13.1	10.3	16.2	13.3	9.9
		4T-2Al (I)[a]	15.8	12.7	8.4	15.7	13.5	7.1
		4T-2Al (II)	16.8	13.7	9.6	15.3	13.3	8.6
		2T[b]	16.7	13.3	10.9			
			16.6 ± 0.8	13.2 ± 0.5	9.8 ± 1.4	15.7 ± 0.5	13.4 ± 0.1	8.5 ± 1.4
	3.0/2.43	4T-lA1	15.7	15.1	13.3	15.0	15.4	14.1
		4T-2Al (I)[a]	17.8	12.6	6.6	15.8	13.7	9.1
		4T-2Al (II)	16.2	13.6	10.8	16.3	12.7	11.8
		$\{2T\}_{2Al}$[c]	15.9	14.1	10.2			
		$\{2T\}_{3Al}$	14.0	15.2	10.3			
			15.9 ± 1.9	14.1 ± 1.5	10.2 ± 3.6	15.7 ± 0.7	13.9 ± 1.2	11.7 ± 2.4
O_3H	47	2T[b]	19.5	13.7	15.1			
	2.43	$\{2T\}_{1Al}$	17.3	14.9	13.9			
		$\{2T\}_{2Al}$[c]	16.7	14.7	13.3			

[a] Roman numbers denote two different hydroxyl groups in the cluster (see Figure 1d). [b] Results taken from ref 24 (Tables 4 and 5). [c] Mean value of all embedding positions of the cluster in lattice is given.

TABLE 3: Deprotonation Energies, ΔE_{DP} (kJ/mol), OH Vibrational Frequencies, ν_{OH} (cm^{-1}) and ^1H NMR Chemical Shifts, $^1\delta_H$ (ppm), of O_1H Groups for Different Clusters nT-mAl and Different Si/Al Ratios

		HF, for given Si/Al of lattice				DFT, for given Si/Al of lattice					
		4T-1Al		4T-2Al		4T-1Al	14T-1Al	4T-1Al	4T-2Al	14T-2Al	4T-2Al
		47.0[a]	3.0	23.0	3.0	47.0[a]	47.0	3.0	3.0	23.0	3.0
ΔE_{DP}	QM/QM-Pot.	1348	1329	1371	1378	1319	1290	1299	1341	1301	1345
	LR//QM-Pot.	−98	−87	−104	−112	−121	−94	−103	−126	−89	−121
	QM-Pot//QM-Pot.	1250	1242	1267	1266	1198	1196	1196	1215	1212	1224
	final $\Delta E^C_{DP} + \Delta$NME[b]	1169	1161	1186	1185	1163	1161	1161	1180	1177	1189
ν_{OH}	QM//QM-Pot.	3596	3621	3605	3604	3623		3634	3625		3637
$^1\delta_H$	QM//QM-Pot.	4.3	3.8	3.9	3.9	4.2		3.8	4.0		3.8

[a] ΔE_{DP} and ν_{OH} data from refs 24 (HF result) and 34 (DFT result). [b] Nuclear motion energy. Zero point energy makes the dominant contribution.

TABLE 4: Deprotonation Energies, ΔE_{DP} (kJ/mol), OH Vibrational Frequencies, ν_{OH} (cm^{-1}), and ^1H NMR Chemical Shifts, $^1\delta_H$ (ppm), of O_1H and O_3H Groups (HF Results) for Different Clusters nT-mAl and Different Si/Al Ratios

		O_1H, for given Si/A1 of lattice and cluster				O_3H, for given Si/Al of lattice and cluster				
		47.0	2.43			47.0	2.43			
		2T[a]	$\{2T\}_{2Al}(1)$	$\{2T\}_{2Al}(2)$	$\{2T\}_{3Al}$	2T[a]	$\{2T\}_{1Al}$	$\{2T\}_{2Al}(1)$	$\{2T\}_{2Al}(2)$	$\{2T\}_{2Al}(3)$
ΔE_{DP}	QM/QM-Pot.	1369	1361	1352	1354	1344	1330	1336	1324	1332
	LR//QM-Pot.	−119	−69	−89	−58	−97	−48	−37	−29	−4
	QM-Pot//QM-Pot.	1250	1292	1264	1296	1247	1282	1299	1295	1328
	final $\Delta E^C_{DP} + \Delta$NME[b]	1169	1211	1183	1215	1166	1201	1218	1214	1247
ν_{OH}	QM//QM-Pot.	3595	3617	3649	3629	3521	3527	3539	3569	3567
$^1\delta_H$	QM//QM-Pot.	4.3	3.8	3.8	3.8	4.7	4.7	4.4	4.3	4.3

[a] Results taken from ref 24 (Table 13). [b] Nuclear motion energy. Zero point energy makes the dominant contribution.

to 14T clusters. As expected,[24] the long-range contribution decreases substantially with increasing cluster size, but the quantum mechanical contribution shows a parallel change of different sign so that the total result stays the same within 3 kJ/mol (DFT results, Table 3). Since the long-range contribution of the embedding potential includes electrostatic and polarization effects, this means that all other contributions, such as delocalization of the anion charge, are already converged at the size of the small embedded cluster.

This is not in favor of the "mean electronegativity" hypothesis of the influence of the Si/Al ratio on the acidity. Our 4T and 14T models have very different Si/Al ratios and, hence, different mean electronegativities. Nevertheless, we calculate the same energy of deprotonation provided that electrostatic and polarization effects are properly taken into account by embedding.

Isolated Brønsted sites, Si(1Al), have nearly constant deprotonation energies, independently of their environment. In the high-silica material, 0 NNN Al, the final deprotonation energy ΔE_{DP} is 1161−1169 kJ/mol (2T and 4T-1Al clusters), while in the low-silica faujasite (1 NNN Al) it is 1161 kJ/mol (4T-1Al cluster). The deprotonation energies of "paired" sites, Si(2Al), are also nearly constant when changing the Si/Al ratio of the embedding lattice and, hence, the number of NNN Al atoms. The changes are 1 and 9 kJ/mol for the HF and DFT results on the 4T-2Al cluster models, respectively (Table 3). Table 3 shows values for one of the two sites of the 4T-2Al model (Figure 1d) since they differ by 2 kJ/mol only. In the high-silica lattice both Al atoms of the "paired" Brønsted sites have 1 NNN Al atom. In the low-silica faujasite they have 2 or 4 NNN Al atoms (Figure 4). However, the Si atom of the Al−

O(H)−Si bridge is always Si(2Al). The deprotonation energies calculated for the 2T cluster models with the same closest environment of the Si atom of the Al−O(H)−Si bridge show some scatter which may be partially due to the small size of the embedded cluster model. Nevertheless, we find that the cluster with the larger number of Al atoms as nearest neighbor to the Si has always the larger deprotonation energy, independently of the size of the cluster and the composition of the lattice into which it is embedded, provided that the same crystallographic site is considered.

The deprotonation energies predicted for the O_1H sites fall into the range 1161−1215 kJ/mol. From shifts of the O_1H stretching frequencies on absorption of CO, values of 1142 and 1161−1177 kJ/mol were inferred for H-USY (Si/Al = 5.7, Na/Al < 0.01) and highly exchanged HY (Si/Al = 2.7, Na/Al = 0.04) zeolites,[21] respectively, in good agreement with our predicted range of values. Attempts to separate the broad OH band of O_1H groups in Na−HY zeolite with Si/Al = 2.56 interacting with aromatic base molecules into several subpeaks yielded deprotonation energies of 1300−1386 kJ/mol which were assigned to Si(1Al)−Si(3Al) sites.[22] These values are higher than our predictions, but the increase of 86 kJ/mol from Si(1Al) to Si(3Al) is close to predicted 54 kJ/mol.

We stress that our calculations predict the existence of acidic sites of various strength in a lattice of a given chemical composition. The main factor governing the acidity is the closest environment of the Brønsted site, i.e. the number of Al atoms in the nearest neighbor tetrahedral position of the Si atom involved in the site, Si(*n*Al). The role of more distant Al atoms (including other NNN Al) is less important and not uniform. This is consistent with the experimental results mentioned in the Introduction. Substituting an Al atom into a lattice of low Al concentration creates strong acidic sites only, "isolated" Si(1Al) sites and the acidity per site remain constant. For a lattice with a high Al concentration additional Al substitution creates weaker and weaker acidic sites. In this case the catalytic activity per Al is expected to decrease.

The Hartree−Fock predictions for the frequencies of isolated O_1H and O_3H groups, 3595 and 3521 cm^{-1}, are about 30 cm^{-1} lower than the values observed for high-silica H-faujasite (Si/Al = 20.7), 3623 and 3550 cm^{-1}.[6] The predicted splitting between the two bands is in excellent agreement with the observed one. The DFT result for the O_1H vibrational frequency is in perfect agreement with experiment.

Figure 6 shows the calculated OH stretching frequencies as a function of the calculated deprotonation energies. Opposed to the deprotonation energy, in the first approximation the O−H stretching frequency is determined by its crystallographic position, O_1H and O_3H in our case, and not by the chemical composition of the lattice. There is a general trend of increasing frequencies with increasing Al content, which is pronounced for the LF band (O_3H) but very weak for the HF band (O_1H), although the scatter is large for the latter case. An increase by 17 cm^{-1} with increasing Al content was also found experimentally for the HF band of HY zeolite (Si/Al = 20.7 to 2.5).[6] For even higher Al content the experiment performed to determine the frequency difference between HF bands of Brønsted sites with Si(4Al) in Na−HX (Si/Al = 1.06) and Si(1Al) atoms in Na−HY (Si/Al = 2.56) zeolites yielded 23 cm^{-1}.[48] We conclude that there is possibly a dependence of the O−H stretching frequency of the bridging hydroxy groups, not only on the number of Al atoms in the closest neighborhood but also on the overall composition of the lattice.

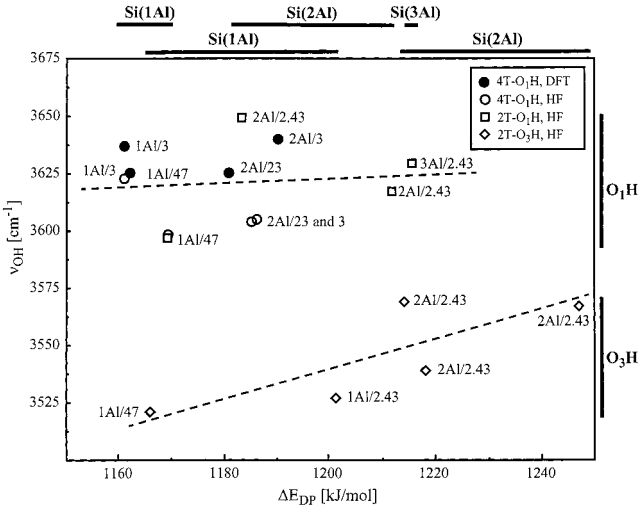

Figure 6. Comparison of the calculated deprotonation energies and O−H stretching frequencies. The *n*Al/*m* labels specify the number of the nearest Al atoms of the Si atom and the Si/Al ratio of the periodic framework considered. The bars at the top mark the ΔE_{DP} regions by a given type of Si(*n*Al) atom for O_1H and O_3H sites, respectively.

The calculations of the ^1H NMR chemical shifts for the isolated Brønsted sites in high-silica faujasite yielded values of 4.2−4.3 ppm for O_1H and 4.7 ppm for O_3H sites (Tables 3 and 4). The chemical shifts calculated for HF and DFT optimized structures are virtually the same thanks to the use of an internal secondary standard. The shifts predicted for O_1H decrease to 3.8−3.9 ppm in low-silica materials. Intermediate values of 3.9−4.0 ppm are predicted for "paired" O_1H Brønsted sites (Si/Al = 23). For O_3H protons a qualitatively different behavior is predicted. The value of 4.7 ppm for the high-silica structure remains the same for isolated sites in high-silica (0 NNN Al atoms, 2T cluster) and low-silica (1 NNN Al atom, $\{2T\}_{1Al}$ cluster) materials. The substitution of Al into a neighbor position of the Si atom has a visible effect on the chemical shift of the O_3H acidic site, which decreases to 4.4 to 4.3 ppm. The role of other NNN Al substitutions seems to be less important. The O_3H sites modeled by $\{2T\}_{2Al}(1)$ and $\{2T\}_{2Al}(3)$ have 3 NNN Al, the one modeled by $\{2T\}_{2Al}(2)$ has 2 NNN Al, but their chemical shifts differ by 0.1 ppm only.

There is almost no correlation between the chemical shift and the acidity measured by the heat of deprotonation if both O_1H and O_3H protons are included (Figure 7). The correlation within each site is better, but the points show a large scatter. For example, the isolated site (4T-1Al cluster) has virtually identical deprotonation energies, both in the high-silica (Si/Al = 47) and the low-silica (Si/Al = 3.0) material, while the ^1H NMR chemical shifts differ as much as 0.5 ppm. In turn, the difference between the deprotonation energies of paired and isolated Brønsted sites in low-silica material (Si/Al = 3.0) is almost 30 kJ/mol, while the chemical shifts are the same. For the O_3H group a deprotonation energy change of 35 kJ/mol for the isolated site going from high-silica to low-silica material is accompanied by virtually no change of the ^1H NMR chemical shift.

The experimental ^1H NMR spectrum of HY faujasite (Si/Al = 2.6) consists of a line at 3.9 ppm and a shoulder at 4.6 ppm.[10] Our calculations confirm that the 3.9 ppm line belongs to the O_1H and the shoulder to the O_3H hydroxyl groups. The ^1H NMR chemical shift of the O_1H groups decreases from 4.4 ppm for Si/Al > 10 (HY) to 3.8 ppm for Si/Al = 1.2 (Na−HX).[11] This change is almost perfectly reproduced by our QM-Pot. embedded cluster calculations. It is consistent with the hy-

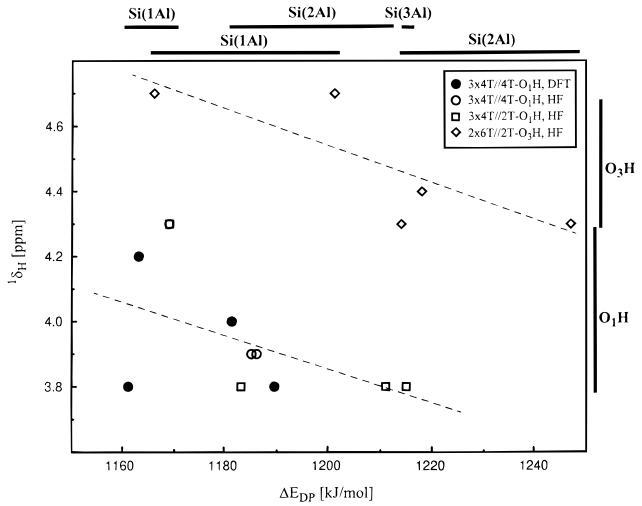

Figure 7. Comparison of the calculated deprotonation energies and ^{1}H chemical shifts. For the explanation of the upper bars see Figure 6.

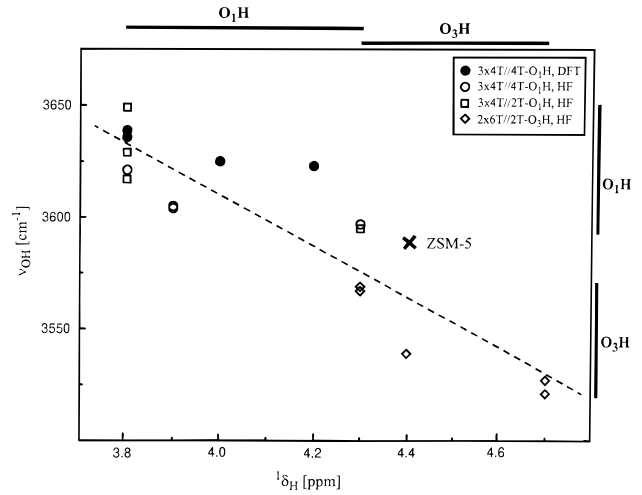

Figure 8. Comparison of the calculated ^{1}H chemical shifts and O−H stretching frequencies.

pothesis that in faujasites of Si/Al > 10 only isolated O_1H Brønsted sites exist (proton shift ∼ 4.3).

A linear correlation between the O−H stretching frequencies and ^{1}H chemical shifts has been proposed on the basis of experimental results.[49,50] Our computed results follow a linear regression with a correlation coefficient of 0.91 (Figure 8)

$$\nu_{OH}\,(cm^{-1}) = 4061.7 - 113.1(^1\delta_H/ppm)$$

in reasonable agreement with the expression derived from experimental data:[50]

$$\nu_{OH}\,(cm^{-1}) = 3884.4 - 68.0(^1\delta_H/ppm)$$

The predicted relation is not limited to the faujasite structures studied. As the cross in Figure 8 indicates, O−H stretching frequencies and ^{1}H chemical shifts predicted for the H-ZSM5 zeolite[24] fit reasonably well into our model.

5. Conclusions

We have shown that the acidity of Brønsted acidic sites in faujasites, measured by the energy of deprotonation, is primarily determined by the Al for Si substitutions in the nearest neighborhood of the Si atom of the Al−O(H)−Si bridge. The role of other NNN Al atoms (NNN Al effect) is less important. Sites of strong acidity, Si(1Al), and weaker ones, Si(2Al) and Si(3Al), coexist in faujasites of low Si/Al ratio. In contrast, O−H stretching frequencies and ^{1}H NMR chemical shifts are in the first approximation determined by the crystallographic position within the lattice, O_1H vs O_3H.

The ^{1}H NMR chemical shifts show a strong dependence on the chemical composition of the lattice, both in their closest vicinity and at further distances. There is no correlation between the proton chemical shifts and the acidities of Brønsted sites. There is a linear relation between the calculated O−H stretching frequencies and ^{1}H chemical shifts which shows good agreement with the experimentally derived relations.

Acknowledgment. This work has been supported by the Max-Planck-Gesellschaft.

References and Notes

(1) Farneth, W. E.; Gorte, R. *J. Chem. Rev.* **1995**, *95*, 615.
(2) Beaumont, R.; Barthomeuf, D. *J. Catal.* **1972**, *26*, 218.
(3) Beaumont, R.; Barthomeuf, D. *J. Catal.* **1972**, *27*, 45.
(4) Beaumont, R.; Barthomeuf, D. *J. Catal.* **1973**, *30*, 288.
(5) Sohn, J. R.; DeCanio, S. J.; Fritz, P. O.; Lunsford, J. H. *J. Phys. Chem.* **1986**, *90*, 4847.
(6) Anderson, M. W.; Klinowski, J. *Zeolites* **1986**, *6*, 455.
(7) Jacobs, P. A.; Uytterhoeven, J. B. *J. Chem. Soc., Faraday Trans. 1* **1973**, *69*, 359.
(8) Datka, J.; Gil, B. *J. Catal.* **1994**, *145*, 372.
(9) Dombrowski, D.; Hoffmann, J.; Fruwert, L. J.; Stock, T. *J. Chem. Soc., Faraday Trans. 1* **1985**, *81*, 2257.
(10) Hunger, M.; Horvath, T.; Engelhardt, G.; Karge, H. G. In *Catalysis by Microporous Materials;* Beyer, H. K., Karge, H. G., Kiricsi, I., Nagy, J. B., Eds.; Studies in Surface Science and Catalysis, Vol. 94; Elsevier: Amsterdam, 1995; p 756.
(11) Freude, D.; Hunger, M.; Pfeifer, H. *Z. Phys. Chem. (Munich),* **1987**, *152*, 171.
(12) Freude, D.; Hunger, M.; Pfeifer, H.; Schwieger, W. *Chem. Phys. Lett.* **1986**, *128*, 62.
(13) Wachter, W. A. In *Theoretical Aspects of Heterogeneous Catalysis;* Moffat, J., Ed.; Van Nostrand Reinhold: New York, 1990; p 110.
(14) Briend, M.; Barthomeuf, D. In *Proceedings of the 9th International Zeolite Conference;* Von Ballmoos, R., et al., Eds.; Butterworth-Heinemann: Montreal, 1992; p 635.
(15) Zhidomirov, G. M.; Kazansky, V. B. *Adv. Catal.* **1986**, *34*, 131.
(16) Gil, B.; Broclawik, E.; Datka, J.; Klinowski, J. *J. Phys. Chem.* **1994**, *98*, 930.
(17) Mortier, W. J. *J. Catal.* **1978**, *55*, 138.
(18) Jacobs, P. A.; Mortier, W. J. *Zeolites* **1982**, *2*, 226.
(19) Dwyer, J.; Fitch, F. R.; Nkang, E. E. *J. Phys. Chem.* **1983**, *87*, 5402.
(20) Sauer, J. *J. Mol. Catal.* **1989**, *54*, 312.
(21) Makarova, M. A.; Al-Ghefaili, K. M.; Dwyer, J. *J. Chem. Soc., Faraday Trans.* **1994**, *90*, 383.
(22) Datka, J.; Broclawik, E.; Gil, B. *J. Phys. Chem.* **1994**, *98*, 5622.
(23) Eichler, U.; Kölmel, C. M.; Sauer, J. *J. Comput. Chem.* **1996**, *18*, 463.
(24) Eichler, U.; Brändle, M.; Sauer, J. *J. Phys. Chem. B* **1997**, *101*, 10035.
(25) Sauer, J. *Chem. Rev.* **1989**, *89*, 199.
(26) Schröder, K.-P.; Sauer, J. *J. Phys. Chem.* **1993**, *97*, 6579.
(27) Klinowski, J.; Radamas, S.; Thomas, J. M.; Fyfe, C. A.; Hartman, J. S. *J. Chem. Soc., Faraday Trans.* **1982**, *78*, 1025.
(28) Czjzek, M.; Jobic, H.; Fitch, A. N.; Vogt, T. *J. Phys. Chem.* **1992**, *96*, 1535.
(29) Sierka, M. Program QMPOT, Humboldt Universität, Berlin, Germany, 1998.
(30) Gale, J. D. *J. Chem. Soc., Faraday Trans.* **1997**, *93*, 629.
(31) Ahlrichs, R.; Bär, M.; Häser, M.; Horn, H.; Kölmel, C. M. *Chem. Phys. Lett.* **1989**, *162*, 165.
(32) Treutler, O.; Ahlrichs, R. *J. Chem. Phys.* **1995**, *102*, 346.
(33) Schröder, K.-P.; Sauer, J. *J. Phys. Chem.* **1996**, *100*, 11043.
(34) Sierka, M.; Sauer, J. *Faraday Discuss.* **1997**, *106*, 41.
(35) Becke, A. D. *J. Chem. Phys.* **1993**, *98*, 5648.
(36) Huzinaga, S. *J. Chem. Phys.* **1965**, *42*, 1293.
(37) Schäfer, A.; Horn, H.; Ahlrichs, R. *J. Chem. Phys.* **1992**, *97*, 2571.
(38) Pulay, P. In *Modern Theoretical Chemistry;* Schaefer, H. F., III, Ed.; Plenum Press: New York, 1977; Vol. 4, p 153.
(39) Rauhut, G.; Pulay, P. *J. Phys. Chem.* **1995**, *99*, 3093.

(40) Dichfield, R. *Mol. Phys.* **1974**, *27*, 789.
(41) Häser, H.; Ahlrichs, R.; Baron, H. P.; Weis, P.; Horn, H. *Theoret. Chim. Acta* **1992**, *83*, 455.
(42) Hase, F.; Sauer, J. *J. Phys. Chem.* **1994**, *98*, 3083.
(43) Chauvel, J. P., Jr.; True, N. S. *Chem. Phys.* **1985**, *95*, 435.
(44) Leslie, M.; Gillian, M. J. *J. Phys. C: Solid State Phys.* **1985**, *18*, 973.
(45) Fuchs, K. *Proc. R. Soc. London Ser. A* **1935**, *151*, 585.
(46) Sauer, J. In *Modeling of Structure and Reactivity in Zeolites;* Catlow, C. R. A., Ed.; Academic Press: London, 1992; p 183.
(47) Sauer, J.; Ahlrichs, R. *J. Chem. Phys.* **1990**, *93*, 2575.
(48) Datka, J.; Broclawik, E.; Gil, B.; Sierka, M. *J. Chem. Soc., Faraday Trans.* **1996**, *92*, 4643.
(49) Kriegsmann, H. *Z. Phys. Chem. (Leipzig)* **1988**, *269*, 178.
(50) Brunner, E.; Karge, H. G.; Pfeifer, H. *Z. Phys. Chem.* **1992**, *176*, 173.